Acta of Bioengineering and Biomechanics
Vol. 15, No. 1, 2013

Original paper
DOI: 10.5277/abb130110

Analysis of wear of polyethylene hip joint cup related to its positioning in patient's body

JACEK ROŃDA*, PAWEŁ WOJNAROWSKI

AGH University of Science and Technology, Faculty of Metals Engineering and Industrial Computing Science, Department of Applied Information Technology and Modelling, al. A. Mickiewicza 30, 30-059 Kraków, Poland.

Polyethylene parts of endoprosthesis are the weakest parts of each medical implant. They can be worn out within several years. During this period, a patient can enjoy good physical efficiency until the wear of polyethylene part limits his/her mobility. Then the reoperation is necessary and positioning of all parts of endoprosthesis has an effect on future patient's mobility and durability of implant. Elements of endoprosthesis during exploitation are heavily loaded both by normal and tangential forces and moments. In this paper, the dependence of wear of polyethylene cup on its positioning in pelvis is the major problem. Wear of the cup is determined by two measures: the depth and volume of a material rubbed off from the contact surface. The sensitivity of the depth of rubbing off is evaluated relative to two angles of anteversion and abduction, and radii of the cup. Numerical results are obtained by using Abaqus FE system with data related to patient's activity identified on the basis of medical reports.

Key words: *hip joint endoprosthesis, wear, coefficient of wear, finite element method*

1. Introduction

Hip joint endoprosthesis replaces the acetabulo-femoral joint, which is the joint between the femur and acetabulum of the pelvis. The primary function of the joint is to support the weight of the body in both static and dynamic postures. The dynamic posture is walking, running or jumping and static one is standing. The joint is composed of a hip prosthesis made of metal, a metal or ceramic head and polyethylene acetabular cup.

Hip joint movements and their ranges, which are preformed by a series of muscles, are listed in Table 1.

A detailed description of the hip joint can be found, e.g., in [1] and [2]. In this paper, movements of the hip joint are analyzed using three planes of motion and the full vector of loading. Previously, two planes and the resultant vector were used for this purpose, as can be seen in [3] and [4]. The Coulomb friction model and the Archard wear equation [5] are applied to evaluation of wear. The Archard model is based on the theory of asperity contact and is used to describe sliding wear of acetabular cup. Numerical results of wear of the polyethylene acetabular cup are obtained using Abaqus FEA suite of software. Recently the FEM has been applied to analysis of various phenomena [6]–[8].

Table 1. Hip joint movements and their ranges

Movements	Ranges of motion from the neutral zero
Lateral or external rotation	30° with the hip extended, 50° with the hip flexed
Medial or internal rotation	40°
Extension or retroversion	20°
Flexion or anteversion	140°
Abduction	50° with hip extended, 80° with hip flexed
Adduction	30° with hip extended, 20° with hip flexed

* Corresponding author: Jacek Rońda, AGH University of Science and Technology, Faculty of Metals Engineering and Industrial Computing Science, Department of Applied Information Technology and Modelling, al. A. Mickiewicza 30, 30-059 Kraków, Poland. Tel: +48 12 617 41 79, fax: +48 12 617 29 21, e-mail: jacekronda@yahoo.co.uk

Received: November 9th, 2011
Accepted for publication: October 17th, 2012

2. Materials and methods

2.1. Contact problem formulation

The contact problem formulation for two bodies: a steel head and a polyethylene acetabular cup, is presented here following [9].

Let us consider two domains: Ω^j, j = 1, 2, where index 1 is assigned to the cup and 2 to the head. The boundary of each body can be split into three surfaces: $\Gamma^j = \Gamma_u^j \cup \Gamma_g^j \cup \Gamma_c^j$.

The displacement field is given on the fraction Γ_u^j of j-body boundary. Γ_g^j is assigned to the fraction of a boundary where the continuous load $g \in (L^2(\Omega^j))^2$ is applied. It is assumed that initially two bodies are in contact with each other on the common part of their boundaries $\Gamma_c = \Gamma_c^1 = \Gamma_c^2$. The body Ω^j is loaded by forces $f^j \in (L^2(\Omega^j))^2$. The normal vector $\mathbf{n}^j$ is directed outward from the domain Ω^j. The friction coefficient η of the contact surface Γ_c fulfils the condition $\eta \geq 0$.

The solution of the two-body contact problem with the Coulomb friction model consists in evaluation of displacement field and stress field $\sigma(u^j)$ which fulfil the following equations and conditions

$$\begin{aligned} &\boldsymbol{\sigma}(\mathbf{u}^j) = \mathbf{D}^j \varepsilon(\mathbf{u}^j) && \text{in} \quad \Omega^j, \\ &\nabla\boldsymbol{\sigma}(\mathbf{u}^j) + \mathbf{f}^j = 0 && \text{in} \quad \Omega^j, \\ &\boldsymbol{\sigma}(\mathbf{u}^j)\mathbf{n}^j = \mathbf{g}^j && \text{on} \quad \Gamma_g^j, \\ &\mathbf{u}^j = 0 && \text{on} \quad \Gamma_g^j, \end{aligned} \tag{1}$$

where $\varepsilon(u^j)$ is the linear tensor of displacement, and $\mathbf{D}^j$ is the elasticity tensor of the fourth order. Equations and conditions (1) are completed by the unilateral contact conditions that must be fulfilled on the contact surface

$$[\mathbf{u}_n] \leq 0, \qquad \boldsymbol{\sigma}_n(u)[\mathbf{u}_n] = 0, \tag{2}$$

where $[\mathbf{u}_n]$ is a drop of the normal component $\mathbf{u}_n$ of displacement measured in the normal direction to the contact surface. The condition (2) is also known as the impenetrability condition. Conditions derived from Coulomb's friction law on Γ_c can be expressed as follows

$$\begin{aligned} &|\boldsymbol{\sigma}_t(u)| \leq \mu |\boldsymbol{\sigma}_n(u)|, \\ &|\boldsymbol{\sigma}_t(u)| \leq \mu |\boldsymbol{\sigma}_n(u)| \Rightarrow [\dot{\mathbf{u}}_t] = 0, \\ &|\boldsymbol{\sigma}_t(u)| \leq \mu |\boldsymbol{\sigma}_n(u)| \Rightarrow \exists \lambda \geq 0, \\ &[\dot{\mathbf{u}}_t] = -\lambda \boldsymbol{\sigma}_t(u), \end{aligned} \tag{3}$$

where $[\dot{\mathbf{u}}_t]$ is a drop of the tangential component of the displacement rate on the boundary Γ_c.

The variational formulation of the problem defined by equations and relations (1), (2) and (3) was presented by Duvaut and Lions [10] and can be expressed as follows

$$\mathbf{a}(\mathbf{u}, \mathbf{v} - \mathbf{u}) + \mathbf{j}(\mathbf{u}, \mathbf{v}) - \mathbf{j}(\mathbf{u}, \mathbf{u}) \geq \mathbf{L}(\mathbf{v} - \mathbf{u}). \tag{4}$$

The inequality (4) is valid for a selected $\mathbf{u} \in K$ and every $\forall \mathbf{v} \in K$. The following denotations are used in (4):

1. K is the convex compact cone of permissible displacements which fulfils impenetrability condition

$$K = \{\mathbf{v} = (\mathbf{v}_1, \mathbf{v}_2) \in \mathbf{V}^1 \times \mathbf{V}^2; [\mathbf{v}_n] \leq 0 \quad \text{on} \quad \Gamma_c\} \tag{5}$$

where

$$\mathbf{V}^j = \{\mathbf{v}^j \in (H^1(\Omega^j))^2, \quad \mathbf{v} = 0 \quad \text{on} \quad \Gamma_u^j\}, \tag{6}$$

2. $\mathbf{a}(\mathbf{u}, \mathbf{v})$ is the quadratic form

$$\begin{aligned} &\mathbf{a}(\mathbf{u}, \mathbf{v}) = \mathbf{a}^1(\mathbf{u}, \mathbf{v}) + \mathbf{a}^2(\mathbf{u}, \mathbf{v}), \\ &\mathbf{a}^j(\mathbf{u}, \mathbf{v}) = \int_{\Omega^j} (\mathbf{D}^j \varepsilon(u^j) : \varepsilon(u^j)) d\Omega, \end{aligned} \tag{7}$$

3. $\mathbf{L}(\mathbf{v})$ is the linear operator

$$\mathbf{L}(\mathbf{v}) = \sum_{j=1}^{2} \int_{\Omega^j} \mathbf{f} \cdot \mathbf{v}^j d\Omega + \int_{\Gamma_u^j} \mathbf{g}^j \cdot \mathbf{v}^j d\Gamma, \tag{8}$$

4. $\mathbf{j}(\mathbf{u}, \mathbf{v})$ is the functional related to the "work of friction"

$$\mathbf{j}(\mathbf{u}, \mathbf{v}) = \int_{\Gamma_c} \mu |\sigma_n(u)| |[\mathbf{v}_t]| d\Gamma. \tag{9}$$

Operators and functionals listed above are defined for all $\mathbf{u}$ and $\mathbf{v}$ which belong to the Sobolev space $(H^1(\Omega))^2$.

2.2. The model of mechanical wear of acetabular cup

Wear of the acetabular cup is evaluated by using Archard's formula, first time proposed in [5] **and still used**, where the volume of worn off surface is given by

$$V = K_f S \| \sigma_n \|, \tag{10}$$

where K_f is Archard's coefficient, S is the slip path, and $\|\sigma_n\|$ is the normal component of stress tensor in contact region.

Formula (10) at the local point of the spherical cup can be written in the incremental form

$$dV = \Delta A dh, \tag{11}$$

where ΔA denotes of element of the apparent contact surface and dh is the infinitesimal depth of wear defined by the expression

$$dh = K_f \| \boldsymbol{\sigma}_n \| dS, \tag{12}$$

which after integration results in

$$h = \int_S K_f \| \boldsymbol{\sigma}_n \| dS. \tag{13}$$

Following [11], the depth of the contact surface wear can be evaluated replacing the norm of vector normal to the contact $|\sigma_n|$ by the product of the contact pressure p_n and the material hardness H

$$h = \int_S K_f \frac{p_n}{H} dS. \tag{14}$$

The coefficient of wear K_f is determined from experimental tests.

2.3. Discrete model of the joint

Finite element model of the hip joint consist of two groups of hexagonal finite elements belonging either to the hip or assigned to the acetabular cup. The FE mesh is shown in Fig. 1.

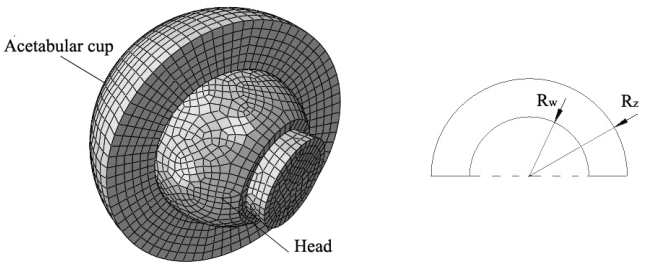

Fig. 1. Discrete model of the hip joint endoprosthesis

Material parameters of UHMWPE polyethylene are given in Table 2 and shown in Fig. 2.

Table 2. UHMWPE material parameters

Young's modulus [MPa]	Poisson's ratio	Density [g/cm^3]
1240	0.4	0.92

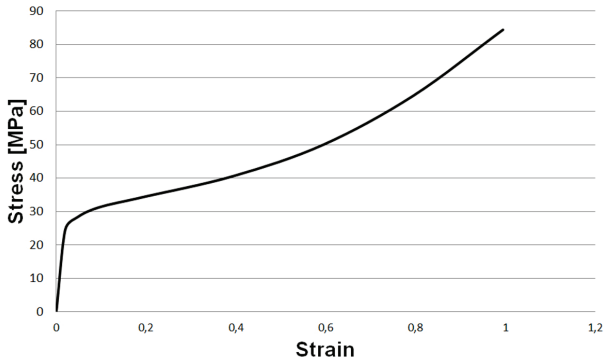

Fig. 2. Stress-strain curve for UHMWPE

Young's modulus and Poisson's ratio are identified on the basis of papers [3], [4], [12]–[15] and analysis of stress-strain curve shown in Fig. 2. The maximum pressure on the cup during the normal human movement ranges between 5 and 8 MPa as mentioned in [4], [13], [16]. Such pressure leads to very small strains, as can be seen in Fig. 2. Following this observation, Young's modulus can be assumed as constant.

The contact problem formulated for the hip joint is solved for three combinations of materials where in all three cases the cup is made of UHMWPE and the head is made either of the CoCrMo alloy or one of two steels marked as Steel 1 or Steel 2. Internal and external radiuses of the cup are given in Table 3.

Table 3. Dimensions of the cup

No.	Diameter [mm]
1	$D_{in} = 22$, $D_{ex} = 46$
2	$D_{in} = 28$, $D_{ex} = 46$
3	$D_{in} = 32$, $D_{ex} = 46$

Coefficients of wear for a hip joint made of various materials are shown in Table 4 and were assumed as constant according to papers [17] and [18]. Results for various numerical models are compared using the coefficient of wear given in paper [3]. This coefficient is related to compression [19], and the relationship is identified following the "pin-of-disk" method and is expressed by

$$K = 2 \times 10^{-6} \sigma^{-0.84}. \tag{15}$$

Table 4. Combination of materials of the tribological pair and wear coefficient [3]

Case no.	Material of the cup	Material of the head	K_f [mm^3/Nm]	Contact environment
1	UHMWPE	CoCrMo	$3.5*10^{-7}$	NaCl solution
2	UHMWPE	Steel	$1.81*10^{-7}$	Animal blood serum
3	UHMWPE	Steel	$8*10^{-7}$	Animal blood serum

The material of a head is assumed as rigid and the only parameter identified for this is the friction coefficient.

2.4. Boundary conditions

The human gait is observed in three rectangular planes: frontal, transverse, and sagittal, as is shown in Fig. 3. The gait data, available from [20] and [21], were used in our numerical evaluations.

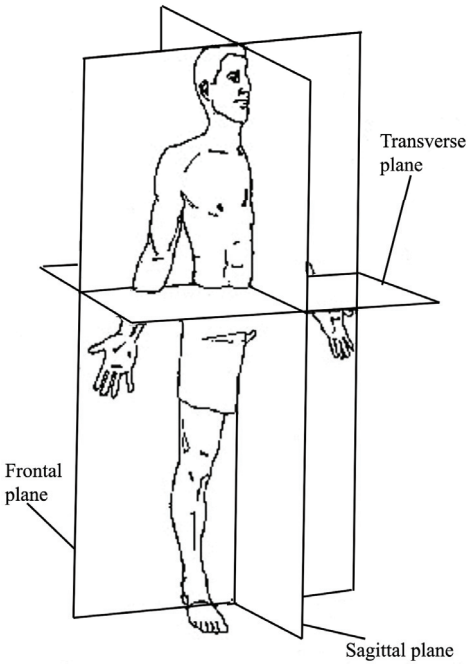

Fig. 3. Human body and its representative rectangular planes

Deflections of the lower limb from the rest position are shown in Fig. 4, where deflections URX, URY and URZ are measured, correspondingly, in the frontal, sagittal and transverse plane.

Three components of loading of the hip joint endoprosthesis are shown in Fig. 5. It is assumed that the cup is durably fixed to the pelvis. The Coulomb friction model with constant coefficient is assumed.

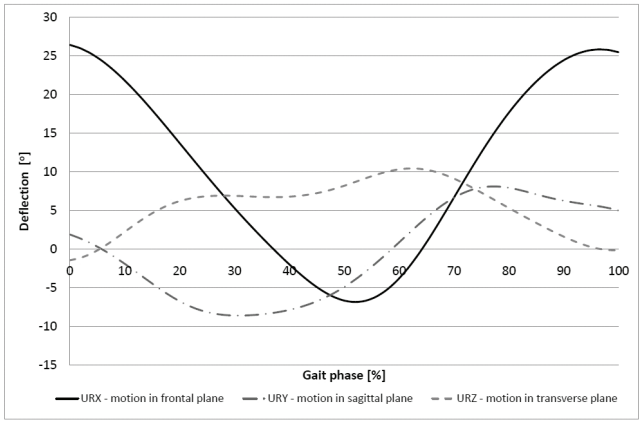

Fig. 4. Deflection of a limb in accordance with gait phase

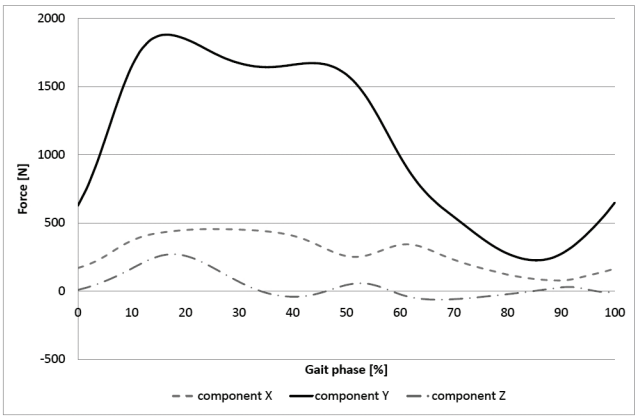

Fig. 5. Variation of hip joint load in accordance with gait phase

3. Results

Following [4], wear is calculated for ten million gait cycles by using commercial finite element Abaqus program. Series of numerical evaluations were conducted to analyze the influence of two angles that determine the position of the cup in the patient's body on wear of the cup. Numerical results are presented for three combinations of materials for the cup–head joint, one value of the anteversion angle of the cup equal to 20°, and three values of the abduction angle: 35°, 45°, and 60°. Three internal diameters of the cup were considered: 22 mm, 28 mm, and 32 mm.

Table 5. Wear of the cup with internal diameter equal to 22 mm

Diameter [mm]	22					
Abduction angle/ Anteversion angle	35°/20°		45°/20°		60°/20°	
Wear parameter / Head–cup joint	Depth of wear [mm/year]	Volume of wear [mm^3/year]	Depth of wear [mm/year]	Volume of wear [mm^3/year]	Depth of wear [mm/year]	Volume of wear [mm^3/year]
CoCrMo UHMWPE	0.082	31.19	0.079	29.85	0.072	27.28
Steel 1 – UHMWPE	0.041	15.80	0.040	15.41	0.035	13.39
Steel 2 – UHMWPE	0.199	75.81	0.194	74.05	0.177	67.59

Table 6. Wear of the cup with internal diameter equal to 28 mm

Diameter [mm]	28					
Abduction angle/ Anteversion angle	35°/20°		45°/20°		60°/20°	
Wear parameter / Head–cup joint	Depth of wear [mm/year]	Volume of wear [mm^3/year]	Depth of wear [mm/year]	Volume of wear [mm^3/year]	Depth of wear [mm/year]	Volume of wear [mm^3/year]
CoCrMo – UHMWPE	0.045	27.55	0.048	29.71	0.049	30.60
Steel 1 – UHMWPE	0.022	13.71	0.024	14.81	0.025	15.26
Steel 2 – UHMWPE	0.111	68.58	0.118	72.90	0.104	64.41

Table 7. Wear of the cup with internal diameter equal to 32 mm

Diameter [mm]	32					
Abduction angle/ Anteversion angle	35°/20°		45°/20°		60°/20°	
Wear parameter / Head–cup joint	Depth of wear [mm/year]	Volume of wear [mm^3/year]	Depth of wear [mm/year]	Volume of wear [mm^3/year]	Depth of wear [mm/year]	Volume of wear [mm^3/year]
CoCrMo – UHMWPE	0.038	30.55	0.038	22.59	0.033	26.38
Steel – UHMWPE	0.019	15.07	0.018	14.75	0.016	13.15
Steel – UHMWPE	0.094	75.78	0.090	72.14	0.082	65.78

The biggest wear is observed for the cup made of UHMWPE with the internal diameter equal to 22 mm and the head made of steel with the coefficient of wear equal to $8*10^{-7}$ mm^3/Nm. The smaller wear appeared for the cup with a diameter of 32 mm and the same conditions as above.

Results of numerical calculation of wear are shown in Tables 5, 6 and 7 for various internal diameters of the cup. Depths of wear are shown in Figs. 6, 7, and 8 and volumes of wear are depicted in Fig. 9, 10 and 11 as a function of the gait number cycles.

It can be noticed from Tables 5, 6, and 7 and Figs. 6, 7, and 8 that the biggest depth of wear occurs for the smallest internal diameter of the cup for each position of the cup in pelvis and for each head. The reason of this high wear rate is that the contact area is smaller and therefore, the contact pressure is the

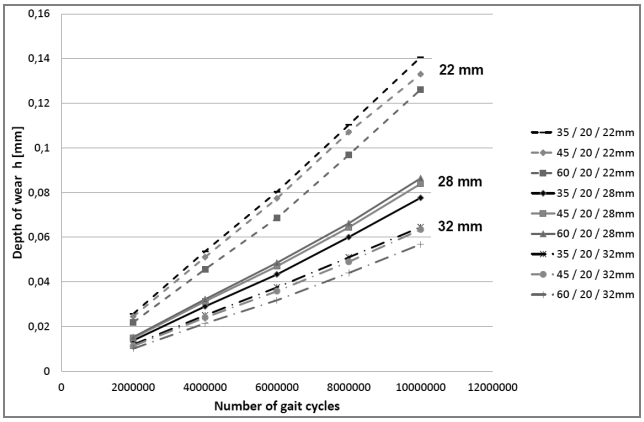

Fig. 6. Depth of wear for the head made of CoCrMo with $K_f = 3.5*10^{-7}$ mm^3/Nm and the cup made of UHMWPE. Lines are marked by numbers in the following order: abduction angle/anteversion angle/internal diameter of the cup

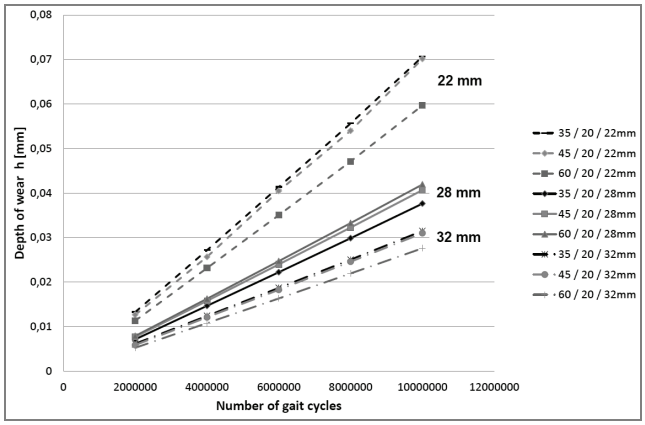

Fig. 7. Depth of wear for the head made of steel with $K_f = 1.81*10^{-7}$ mm^3/Nm and the cup made of UHMWPE. Lines are marked by numbers in the following order: abduction angle/anteversion angle/internal diameter of the cup

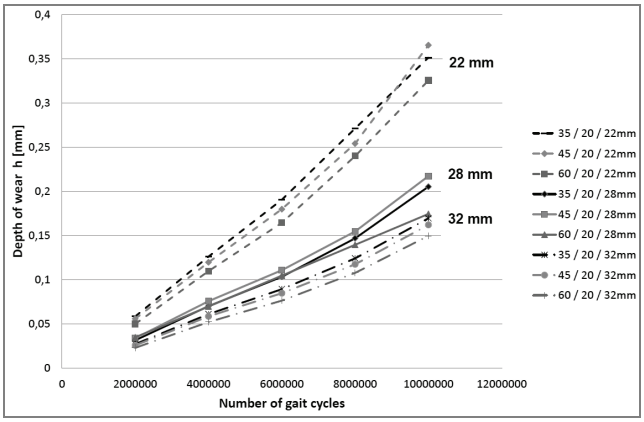

Fig. 8. Depth of wear for the head made of steel with $K_f = 8*10^{-7}$ mm^3/Nm and the cup made of UHMWPE. Lines are marked by numbers in the following order: abduction angle/anteversion angle/internal diameter of the cup

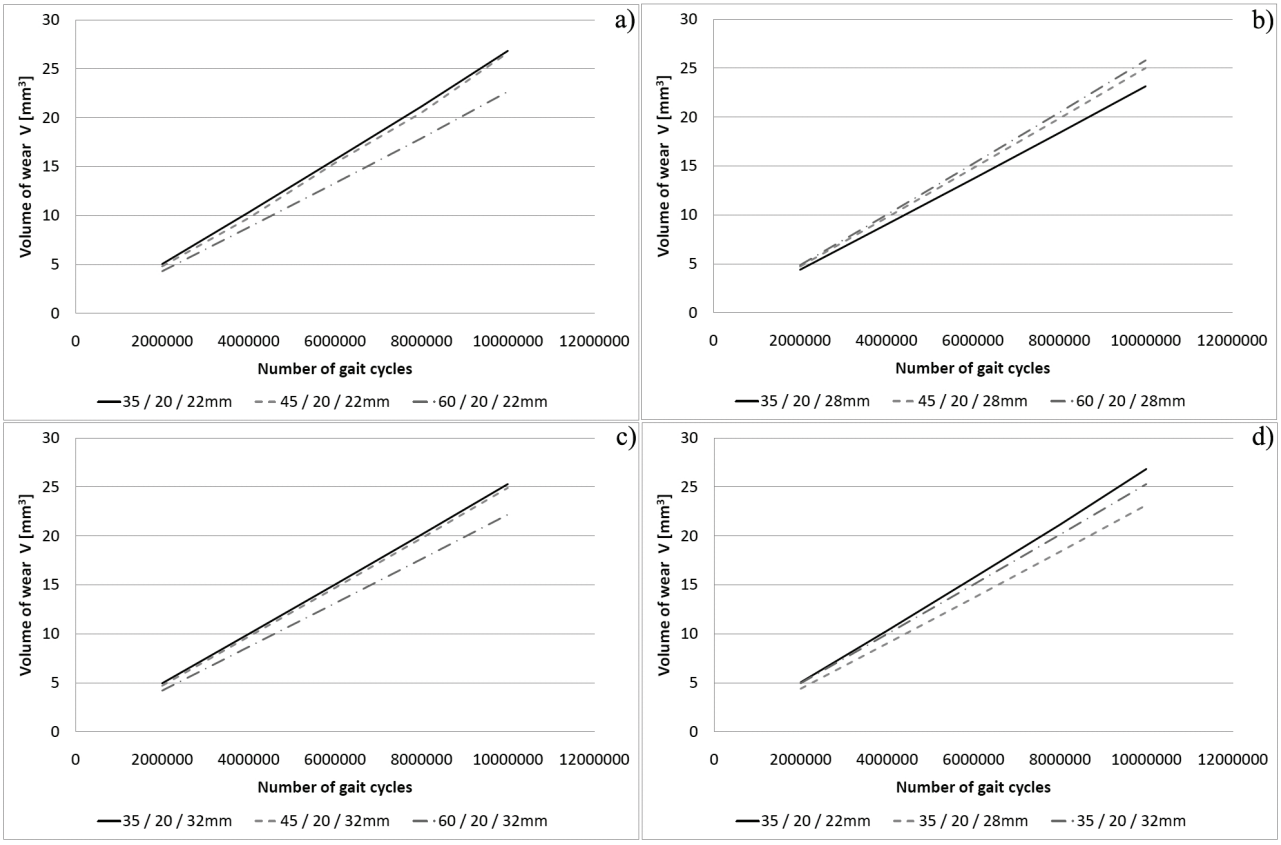

Fig. 9. Volume of wear for the head made of CoCrMo with $K_f = 3.5*10^{-7}$ mm^3/Nm and the cup made of UHMWPE. Lines are marked by numbers in the following order: abduction angle/anteversion angle/internal diameter of the cup. Diagrams are grouped according to the internal diameter of the cup. Part (d) is for the comparison of wear for various internal diameters of the cup

biggest for the same load, i.e., weight of a patient. It can also be observed that values of the depth wear for various materials of the head vary up to 2.74 times comparing the point corresponding to 10 mln cycles on lines marked by 45/20/22 in Figs. 8 and 6. But the ratio of wear coefficients is almost the same and equals 8/3.5 = 2.28. The biggest difference in wear measured by the volume of wear at the point corresponding to 10 mln cycles can be observed for lines marked by 35/20/22 in Fig. 11 and 9.

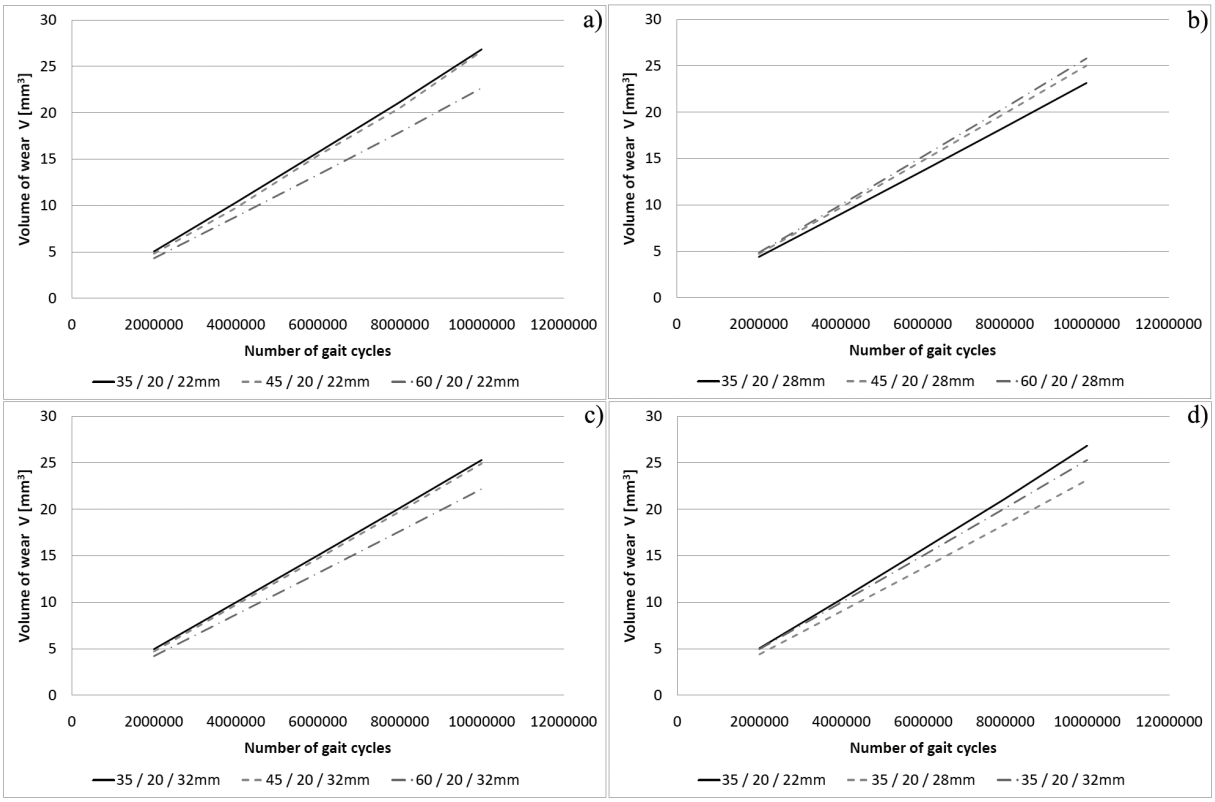

Fig. 10. Volume of wear for the head made of Steel with $K_f = 1.81*10^{-7}$ mm^3/Nm and the cup made of UHMWPE. Lines are marked by numbers in the following order: abduction angle/anteversion angle/internal diameter of the cup. Diagrams are grouped according to the internal diameter of the cup. Part (d) is for the comparison of wear for various internal diameters of the cup

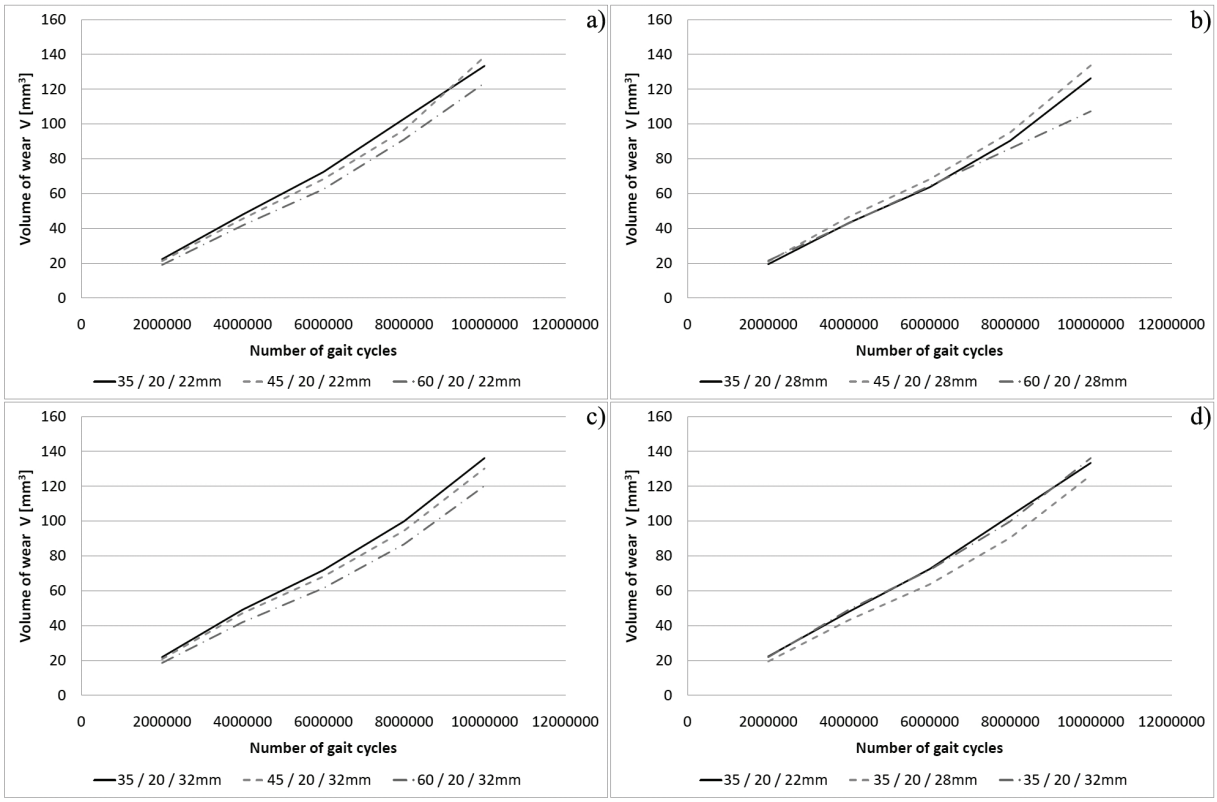

Fig. 11. Volume of wear for the head made of Steel with $K_f = 8*10^{-7}$ mm^3/Nm and the cup made of UHMWPE. Lines are marked by numbers in the following order: abduction angle/anteversion angle/anternal diameter of the cup. Diagrams are grouped according to the internal diameter of the cup. Part (d) is for the comparison of wear for various internal diameters of the cup

Table 8. Comparison of the annual average depth of wear for cups

	Depth of wear [mm/year]			
UHMWPE cup combined with the head made of the following materials	Clinical trials	Wear of cup measured on the mechanical simulator	Wear evaluated in [3]	Wear evaluated by the authors by using Abaqus
	Diameter 22 mm			
CoCrMo	–	–	–	0.079
Steel (1)	–	–	0.029	0.040
Steel (2)	0.623	0.150	0.111	0.194
	Diameter 28 mm			
CoCrMo	0.247	0.091	0.037	0.048
Steel (1)	–	–	0.019	0.024
Steel (2)	0.200	0.108	0.111	0.118
	Diameter 32 mm			
CoCrMo	–	0.053	0.036	0.038
Steel (1)	–	–	0.021	0.018
Steel (2)	0.320	0.036 – 0.059	0.073	0.090

Numerical results for the annual average wears of the cup are compared in Table 8 with experimental results taken from [3].

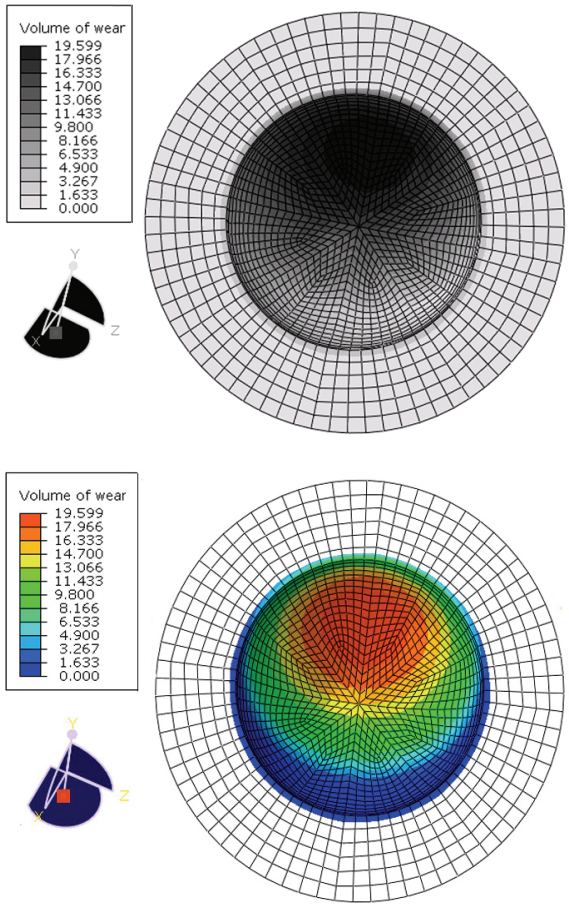

Fig. 12. Maps of the volume of wear of the cup for abduction angle of 45°, and anteversion angle of 20°. The cup is made of UHMWPE and the head is made of CoCrMo. The contact diameter is 28 mm

Maps of wear volume for the cup made of UHMWPE with the internal diameter equal to 28 mm are shown in Fig. 12 for the angle of abduction: 45° and the angle of anteversion: 20°, and the head made of CoCrMo.

4. Discussion

A finite element method was proposed for estimation of wear appearing in artificial hip joint based on Archard's wear law. The wear behavior for Archard's model depends on contact stresses, sliding distance and coefficient of wear. It is well known from the literature that the basic polyethylene wear depends on several factors, including the patient's activity level, diameter of the head and acetabular cup, orientation of the cup in the pelvis, design and quality of ultra-high molecular weigth polyethylene, and sterilization method. Scifert et al. [22] reported the position of the acetabular cup in terms of abduction and anteversion angles, which was shown to affect both the range of motion and stability. The present study demonstrates that the orientation of the acetabular cup also affects polyethylene wear in the hip joint endoprosthesis.

Numerical results are presented for one value of the anteversion angle of the cup equal to 20°, and three values of the abduction angle: 35°, 45°, and 60°. Three internal diameters of the cup were considered: 22 mm, 28 mm, and 32 mm. The model used in the present study was based on Archard's wear law and elasto-plastic polyethylene properties. After calculating contact stresses and sliding distance, the wear

depth was calculated and the acetabular surface geometry was modified to calculate wear for a new gait cycle.

The wear depths were very similar to those reported by Maxian et al. [23], Hung et al. [3], and Capitanu et al. [4]. In their study, UHMWPE-CoCrMo materials were applied for the cup and head components. For example, for acetabular cup with a 28 mm inner diameter that was oriented at 45° of abduction angle and 15° anteversion angle, Maxian et al. [23] reported a mean linear wear rate from 0.037 to 0.111 mm/year. In the present study, the mean wear of depth for the same orientation for abduction angle and different orientation for anteversion angle was 0.048 mm/year. Capitanu et al. [4] reported the mean volume of wear of 28.17 mm^3/year, i.e., 0.047 mm/year. In the present study, the mean volume of wear was 29.71 mm^3/year. With the acetabular abduction angle increasing the mean wear of depth increased by about 8%, for a 28 mm inner diameter cup and decresed by about 10% for cups of 22 and 32 mm inner diameter. Patil et al. [24] reported changing the abduction and anteversion angles. For example, for the change of abduction angle from 45° to 55°, the wear of depth increased by 5% to 8%, depending on the anteversion angle. Hung et al. [3] presented only one variant of acetabular orientation in the pelvis, but shown for three cases of the cup inner diameter and three different materials for the head. Numerical results of the annual mean wear of the cup are compared in Table 8. The difference between the works presented is related to the different assumptions made for numerical models of the hip joint endoprothesis. In the present study, it was assumed that the forces and the range of motion are in three planes. Papers [3], [4], [23], [24] were limited to the resultant force vector and the range of motion of the flexion/extension plane only. The differences in assumptions certainly affect the sensitivity of results. It is important for numerical models that errors resulting from numerical calculations be eliminated, which may also affect the size of the depth of wear.

The finite element analysis is an attractive option to initially explore the effect of changing parameters, but should be valid with experimental tests. The finite element numerical model of wear simulation is an efficient and inexpensive means of evaluating the effect of important factors on wear. However, any significant predictions made by the numerical model need to be validated. This can be done by using hip joint simulators in the laboratory and testing actual endoprosthesis under carefully controlled conditions. The laboratory model of wear simulation is more valid than numerical one because it replaces some of the simplified assumptions with actual experimental conditions. Another challenge for authors is to perform experiments using a hip joint simulator for valid results.

5. Conclusions

Wear of the acetabular cup depends on the following factors:

1) surface layers in contact for a cup made of UHMWPE and a head usually made of steel or CoCrMo,

2) friction coefficients and wear of the friction pair: head–cup,

3) cup positioning in the pelvis measured both by the abduction and the anteversion angles,

4) the number of gait cycles and patient's weight,

5) contact area defined by the contact radius and diameter of contact area related to an internal radius of the cup,

Depths of wear evaluated by the authors by applying FE program Abaqus are compared in Table 8 with corresponding measures of wear evaluated either by clinical experiments or tests conducted on mechanical simulators or data taken from [3]. Average values of wear evaluated by FEM and measured from simulator tests are similar but unfortunately different from the data specified by clinical tests. The major reason of this discrepancy between numerical and clinical results is poor identification of real patient's activity that influences the identification of loading history. An undefined dynamics of motion could be another reason of this variance.

Discrepancies between results of clinical experiments and tests of wear either conducted on simulators or generated by FEM calculations can be due to simplifications applied in phenomenological models, i.e., material models and material characteristics. In particular, the ultra-high density polymer (UHMPWE) is assumed here to be elasto-plastic material with material characteristics shown in Table 2 which were identified following results presented in [3], [4], [12]–[15].

The distribution of compression on the cup surface evaluated in this paper is similar to that published before but our paper includes pre-setting of the polyethylene acetabular cup. Following [3], it is assumed that the wear coefficient is constant which leads to further discrepancies between numerical and experimental results. In future investigations of wear the wear coefficient should be related to the contact stress.

However, regardless of how difficult the task is, we are going to improve the identification of the contact surface loading and reevaluate the hip joint contact problem following utilization of data extracted from clinical tests planned strictly for the needs of our research.

Acknowledgements

The numerical model was developed under the grant MNiSW/IBM_BC_HS21/AGH/072/2010.

References

[1] SYLWANOWICZ W., MICHAJLIK A., RAMOTOWSKI W., *Anatomia i fizjologia człowieka*, Państwowy Zakład Wydawnictw Lekarskich, Warszawa, 1991.

[2] BĘDZIŃSKI R., KĘDZIOR K., KIWERSKI J., MORECKI A., SKALSKI K., *Biomechanika i inżynieria rehabilitacyjna*, Biocybernetyka i Inżynieria Biomedyczna 2000, tom 5, Akademicka Oficyna Wydawnicza Exit, Warszawa, 2004.

[3] HUNG J.P., WU S.S.J., *A comparative study on wear behavior of hip prosthesis by finite element simulation*, Biomedical Engineering: Applications, Basis and Communications, 2002, 14, 139–148.

[4] CAPITANU L., ONISORU J., IAROVICI A., *Wear prediction of hip endoprostheses*, The Annals of University "Dunarea De Jos" of Galati, 2007, Fascicle VIII, 39–44.

[5] ARCHARD J.F., *Contact and Rubbing of Flat Surfaces*, J. Appl. Phys., 1953, 24, 981–988.

[6] HYRCZA-MICHALSKA M., ROJEK J., FRUITOS O., *Numerical simulation of car body elements pressing applying tailor welded blanks – practical verification of results*, Archives of Civil and Mechanical Engineering, 2010, 10(4), 31–44.

[7] JOVICIC G., ZIVKOVIC M., SEDMAK A., JOVICIC N., MILOVANOVIC D., *Improvement of algorithm for numerical crack modelling*, Archives of Civil and Mechanical Engineering, 2010, 10(3), 19–35.

[8] TRZEPIECIŃSKI T., *3D Elasto-plastic FEM analysis of the sheet drawing of anisotropic steel sheet metals*, Archives of Civil and Mechanical Engineering, 2010, 10(4), 95–106.

[9] BAILLET L., SASSI T., *Mixed finite element formulation in large deformation frictional contact problem*, Revue Europeenne des Elements Finis, 2005, 14, 287–304.

[10] DUVAUT G., LIONS J.L., *Inequalities in mechanics and physics*, Springer-Verlag, Berlin, New York, 1976.

[11] CHMIEL A., *Finite element simulation methods for dry sliding wear*, Master's thesis, Air Force Institute of Technology, Ohio, 2008.

[12] KOWALEWSKI P., WIELEBA W., *Sliding polymers in the joint alloplastic*, Archives of Civil and Mechanical Engineering, 2007, 7(4), 107–119.

[13] GOREHAM-VOSS C., HYDE P.J., HALL R.M., FISHER J., BROWN T.D., *Cross-shear implementation in sliding-distance-coupled finite element analysis of wear metal-on-polyethylene total joint arthoplasty: intervertebral total disc replacement as an illustrative application*, Journal of Biomechanics, 2010, 43(9), 1674–1681.

[14] IMBERT L., *Working principle of dual mobility (total hip replacement): wear and design optimization*, Diploma work no 64/2011, Chalmers University of Technology, Goteberg, Sweden, 2011.

[15] SHIN J., LEE D., KIM S., JEONG D., LEE H.G., KIM J., *The effects of mesh style on the finite element analysis for artificial hip joints*, The journal of the Korean Society for Industrial and Applied Mathematics, 2011, 15(1), 57–65.

[16] PIETRABISSA R., RAIMONDI M., DI MARTINO E., *Wear of polyethylene cups in total hip arthroplasty: a parametric mathematical model*, Medical Engineering and Physics, 1998, 20, 199–210.

[17] PENMETSA J., LAZ P.J., PETRELLA A.J., RULLKOETTER P.J., *Influence of Polyethylene Creep Behavior on Wear in Total Hip Arthroplasty*, Journal of Orthopaedic Research, 2006, 24, 422–427.

[18] SFANTOS G.K., ALIABADI M.H., *Total hip arthroplasty wear simulation using boundary element method*, Journal of Biomechanics, 2007, 40, 378–389.

[19] VASSILIOU K., UNSWORTH A., *Is the wear factor in total joint replacements dependent on the nominal contact stress in ultra-high molecular weight polyethylene contacts?* Journal of Engineering in Medicine, 2004, 218(2), 101–107.

[20] BŁASZCZYK J.W., *Biomechanika kliniczna. Podręcznik dla studentów medycyny i fizjoterapii*, Wydawnictwo Lekarskie PZWL, Warszawa, 2004.

[21] HELLER M.O., BERGMANN G., DEURETZBACHER G., DÜRSELEN M., POHL M., CLAUS L., HAAS N.P., DUDA G.N., *Musculo-skeletal loading conditions at the hip during walking*, Journal of Biomechanics, 2001, 34(7), 883–893.

[22] SCIFERT C., BROWN T., PEDERSEN D., CALLAGHAN J., *A finite element analysis of factors influencing total hip dislocation*, Clinical Orthopaedics and Related Research, 1998, 355, 152–162.

[23] MAXIAN T., BROWN T., PEDERSEN D., CALLAGHAN J., *A sliding-distance-coupled finite element formulation for polyethylene wear in total hip arthroplasty*, Journal of Biomechanics, 1996, 29(5), 687–692.

[24] PATIL S., BERGULA A., CHEN P., COLWELL C., D'LIMA D., *Polyethylene wear and acetabular component orientation*, The Journal of Bone and Joint Surgery, 2003, 85A(4), 56–63.